Journal of Crystal Growth 571 (2021) 126244

Contents lists available at ScienceDirect

Journal of Crystal Growth

journal homepage: www.elsevier.com/locate/jcrysgro

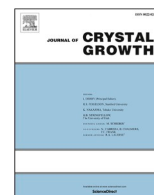

Effect of step edges on the adsorption behavior on vicinal AlN(0001) surface during metal-organic vapor phase epitaxy: *An ab initio study*

Toru Akiyama *, Takumi Ohka, Katsuya Nagai, Tomonori Ito

Department of Physics Engineering, Mie University, 1577 Kurima-Machiya, Tsu 514-8507, Japan

A R T I C L E I N F O

Communicated by Gen Sazaki

Keywords:
A1. Computer simulation
A1. Adsorption
A3. Metalorganic vapor phase epitaxy
B1. Nitrides
B2. Semiconducting III-V Materials

A B S T R A C T

We present systematic theoretical investigations for the adsorption behavior of Al and N adatoms on vicinal AlN (0001) surface under metal–organic vapor phase epitaxy (MOVPE) growth condition by means of *ab initio* electronic structure calculations. Prior to the investigation adatoms, we reveal the growth condition dependence of stable structure for bilayer step edges during the MOVPE. The vicinal surface with hydrogen terminated N atom and NH_2 (N-H + Al-NH_2) is found to be the most stable under N-rich limit whereas the surface with hydrogen terminated N atom (N-H + Al-H) with NH_2 at the step edge is favorable over the wide range of Al chemical potential. This suggests that N-H + Al-NH_2 and N-H + Al-H with NH_2 at the step edge appear at high and low temperatures, respectively. For both surface models, we also elucidate that the adsorption energy of Al adatoms at the step edge is much lower than that in the terrace region, indicating that Al adatoms are easily incorporated into the step edge. The estimated values of Ehrlich-Schwöbel barrier (ESB) of Al adatoms for N-H + Al-NH_2 and N-H + Al-H with NH_2 at the step edge are −1.4 and −1.9 eV, respectively. The relationship between the adsorption behavior and surface morphology during the MOVPE is discussed on the basis of calculated ESB as well as adsorption energies and migration barriers.

1. Introduction

The surface morphology plays an important role to fabricate electronic and optoelectronic devices in group-III nitrides including AlN and GaN [1–9]. It has been well known that the growth parameters such as growth temperature and V/III ratio are crucial to control AlN surface morphology including step-bunching and step-flow in epitaxial growth by metal–organic vapor phase epitaxy (MOVPE). For instance, the step-bunching occurs at high temperature of 1250 °C [8] and low V/III ratio [9]. Furthermore, the phase diagram separating step-flow and step-bunching as functions of V/III ratio and substrate off angle in the MOVPE of AlN has been successfully achieved recently [8,9]. These surface morphologies are consequence of the kinetic effects of epitaxial growth process on the surface including step edges. Particularly, Ehrlich-Schwöbel barrier (ESB) [10,11], which is an additional diffusion barrier crossing down the step and attach to the lower step edge, is a decisive factor for the morphology. The presence of ESB induces the asymmetry in adsorption and migration of adatoms, which results in various interesting surface phenomena such as step meandering and bunching [12–15]. However, there are very few studies for the growth behavior of stepped AlN(0001) surfaces during MOVPE from atomistic viewpoint. The relationship between ESB and resultant morphology on AlN(0001) surface during MOVPE has never been examined by theoretical approach using *ab initio* calculations.

On the baisis of *ab initio* calculations, we have previously studied the adsorption and desorption behavior on reconstructed GaN(0001) and AlN(0001) surfaces during epitaxial growth such as molecular beam epitaxy and MOVPE. We have elucidated specific features of adatom behavior which depends on the growth parameters such as growth pressure and temperature [16,17]. More recently, we have performed comprehensive and systematic calculations to elucidate the adsorption behavior of adatoms on vicinal GaN(0001) surface by means of *ab initio* calculations [18–20]. It has been revealed that the adsorption and migration behavior of gallium and nitrogen adatoms strongly depends on the reconstructions including the atomic arrangements of step edges. For the gallium adatom, the single-layer step edge tends to incorporate the adatom and an inverse ESB has been obtained. We have inspected the difference in the surface morphology during MOVPE in terms of the calculated adsoprion energy, migration barriers and ESB on the vicinal surfaces. In this study, we extend our theoretical study to clarify the

* Corresponding author.
E-mail address: akiyama@phen.mie-u.ac.jp (T. Akiyama).

https://doi.org/10.1016/j.jcrysgro.2021.126244
Received 2 March 2021; Received in revised form 24 May 2021; Accepted 1 July 2021
Available online 7 July 2021
0022-0248/© 2021 Elsevier B.V. All rights reserved.

effects of step edges of vicinal AlN(0001) surface taking account of MOVPE condition on the growth kinetics. Here, we assume that Al and N atoms decomposed from source gases such as trimethylaluminum and NH_3 mainly contribute to the growth during MOVPE. The behavior of aluminum and nitrogen adatoms for vicinal AlN(0001) surfaces taking account of the MOVPE condition is verified on the basis of theorerical approarch using *ab initio* calculations. The relationship between ESB and AlN surface morphology under MOVPE condition is also discussed.

2. Methodology

In this study, the surfaces with step edges during MOVPE are simulated by vicinal slab models with (2 × 9) periodicity, which is constructed by six bilayers AlN with artificial H atoms terminating bottom surface [21]. The interactions between adjacent slabs are eliminated by including 15 Å vacuum region in the slab model. Details of slab geometry is described elsewhere [18,20]. Fig. 1 shows typical atomic configurations at the step edge as well as terrace region considered in this study. The step edge is constructed by a bilayer step, which has been reported by the atomic force microscopy (AFM) observations [8]. The geometry of the ideal surface is shown in Fig. 1(a). In addition, we construct various models, which are inferred by the electron counting (EC) rule [22] and surface reconstructions on planar one under MOVPE growth condition in previous calculations [16,17,23–26]. In the slab models taking account of the reconstruction, we adopt a terrace region whose periodicity is a multiples of the (2 × 2) surface unit cell which is required to satisfy the EC rule. Therefore, one (2 × 8) terrace region and a bilayer layer step constitutes periodic (2 × 9) vicinal slabs. For the reconstructions under extreme Al-rich condition, the surface covered by 1 monolayer (ML) excess Al (Al adlayer) shown in Fig. 1(b) is taken into account. For the MOVPE growth on planar AlN(0001) surface, there are many reports for reconstructed structures with H atoms and NH_2 [16,17,23–26]. According to previous calculations, we make considerations of hydrogen terminated surface (3Al-H) shown in Fig. 1(c), which is taken from the (2 × 2) surface with three Al–H bonds. Furthermore, we take hydrogen terminated surfaces with pre-adsorbed N atoms shown in Fig. 1(d) into account according to the (2 × 2) surface with a Al–H bond and hydrogen terminated N adatom, which becomes stable under intermediate condition with high H_2 pressure ambient. The surface with both hydrogen terminated N atom and NH_2 (N-H + Al-NH_2) shown in Fig. 1(e) is also considered. This comes from the stable (2 × 2) surface under N-rich with high H_2 pressure ambient. For each reconstructions, various atomic arrangements at the step edge are examined. For instance, we consider NH_2 and NH groups attaching the step edge, as shown in Fig. 1(f). We examine in total 14 different cofigurations including the surfaces without H atoms, which are based on the (2 × 2) reconstructions with either N or Al atom in Ref. [19].

We perform *ab initio* calculations within density functional theory using pseudopotential approach with plane-wave basis set. For exchange–correlation functionals of valence electrons, we use the generalized gradient approximation [27]. To simulate nuclei and core electrons, norm-conserving pseudopotentials [28] are used for Al and H atoms and ultrasoft pseudopotential [29] is used for N atoms. The plane-wave basis set with a cut-off energy of 30.25 Ry is employed to expand the valence wave functions. The conjugate-gradient technique [30,31] is utilized for both electronic structure calculation and geometry optimization. The calculated lattice parameters of AlN (a = 3.12 Å and c = 5.02 Å) with wurtzite structure coincide with the experimental data [32]. We have carried out the computations using extended Tokyo *Ab initio* Program Package (xTAPP) [33,34].

To evaluate the stability of vicinal surfaces, the formation energy E_{form} is evaluated as a function of Al chemical potential μ_{Al}. The formation energy is defined as

$$E_{form}(\mu_{Al}) = E_{tot} - E_{ref} - (n_{Al} - n_N)\mu_{Al} - n_N E^{bulk}_{AlN} - n_H\mu_H, \quad (1)$$

where E_{tot} is the total energy of the slab under consideration, E_{ref} is the total energy of the slab for reference, and E^{bulk}_{AlN} is the total energy of bulk AlN per formula unit. Here, we set the reference surface as the vicinal surface shown in Fig. 1(a). The number of either excess or deficit atoms compared with the reference are described by n_{Al}, n_N and n_H for aluminum, nitrogen, and hydrogen, respectively. The equilibrium condition for μ_{Al} and N chemical potential (μ_N) for the crystal growth, which is expressed as $\mu_{Al} + \mu_N = E^{bulk}_{AlN}$, is used. It should be noted that there is a thermodynamically allowed range in μ_{Al}. The upper (lower) limit in μ_{Al} corresponds to Al-rich (N-rich) condition. The energy range of μ_{Al} is equivalent to the formation enthalpy $\Delta H_f = E^{bulk}_{AlN} - E^{fcc-Al}_{tot} - E^{N_2}_{tot}$, where $E^{N_2}_{tot}$ and E^{fcc-Al}_{tot} are the total energies (per atom) of N_2 molecule and fcc

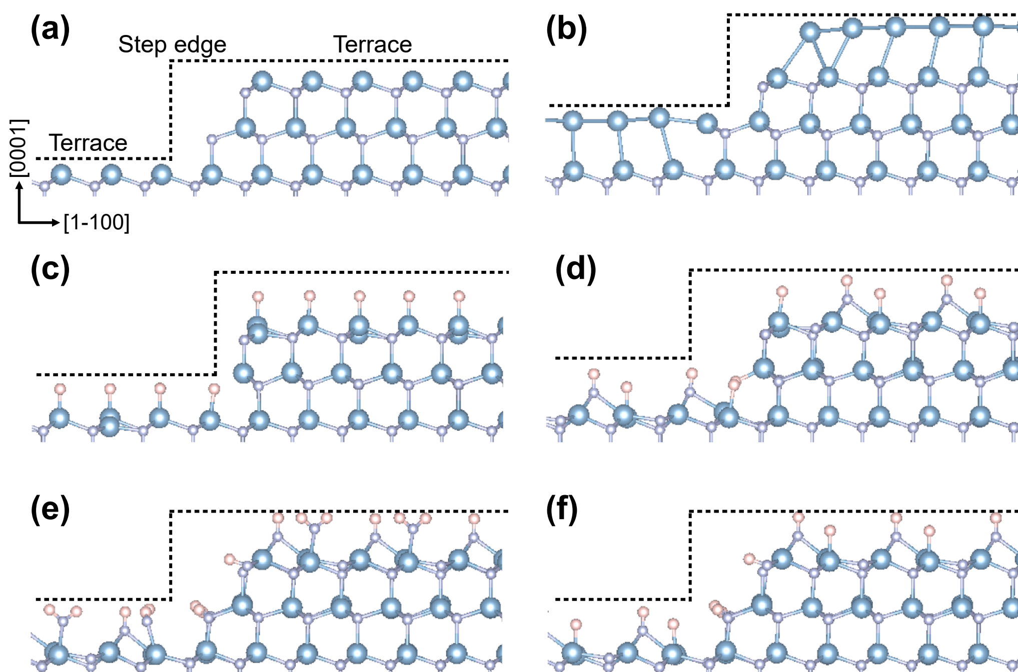

Fig. 1. Side views along the [1$\bar{1}$00] and [0001] directions of slab models for (2 × 9) vicinal surface with bilayer step edge for (a) ideal surface, and the reconstructed surface with (b) one monolayer (ML) excess aluminum atoms (Al adlayer), (c) hydrogen atoms (3Al-H), (d) hydrogen terminated nitrogen atoms (N-H + Al-H), (e) hydrogen terminated nitrogen atoms and amino group (N-H + Al-NH_2), and (f) N-H + Al-H with amino group at the step edge. Aluminun, nitrogen, and hydrogen atoms are represented by blue, purple, and pink circles, respectively. Step edge and terrace regions are indicated by dashed stepwise lines. Periodic boundary condition are imposed and the unit cell includes one bilayer step edge with 5.24 Å height.

Al. The range of μ_{Al} is therefore described as $\mu_{Al}^{fcc} + \Delta H_f \leqslant \mu_{Al} \leqslant \mu_{Al}^{fcc}$, where μ_{Al}^{fcc} is the chemical potential of fcc Al. The calculated ΔH_f for AlN is -2.80 eV, reasonably consistent with the experimental value [35]. Moreover, for hydrogen chemical potential μ_H we here assume H-rich condition corresponding to MOVPE growth using H_2 carrier gas. The H-rich condition is set by the gas phase chemical potential of H atoms to the experimental condition. We employ the value corresponding to H_2 molecule for pressure at 76 Torr and 1370 K written as $\mu_H - \mu_{H_2} = -1.05$ eV, where μ_{H_2} denotes the chemical potential (per atom) for single H_2 molecule at 0 K. The adsorption behavior on the vicinal (2×9) surface along the $[1\bar{1}00]$ direction is obtained by constructing one-dimensional energy mapping in which the adatom is fixing at a certain initial position in the $[1\bar{1}00]$ direction and allowing the relaxation of the other atoms. The mapping of adsorption is accomplished by sample the adsorption energies at various positions. 27 equidistant linear positions along the $[1\bar{1}00]$ direction are chosen in total. To determine the initial position of adatoms at each position of vicinal surfaces along the $[112^{-}0]$ direction, we also perform the calculations of adatom on planar AlN(0001) surface using the (2×2) slab model. In addition to the calculated results on planar AlN(0001) surface, the calculations for various positions along the $[1\bar{1}20]$ direction are furthermore performed at the step edges. We calculate the adsorption energy E_{ad} from the total energy difference between the vicinal surfaces with and without adatom. The origin of the adsorption energy corresponds to the energy of the surface with adatom in vacuum region at 0 K.

3. Results and discussion

Fig. 2 shows the calculated formation energy using Eq. (1) for various vicinal (2×9) surfaces as a function of Al chemical potential μ_{Al}. The calculated formation energies clearly demonstrate that the stable structure of the vicinal surface is dependent on Al chemical potential. The N-H + Al-H with NH_2 at the step edge shown in Fig. 1(f) has the lowest $E_{form}(\mu_{Al})$ and is stabilized in the wide range of μ_{Al}. This is ranging from -2.15 to -0.90 eV. In contrast, N-H + Al-NH_2 shown in Fig. 1(e)

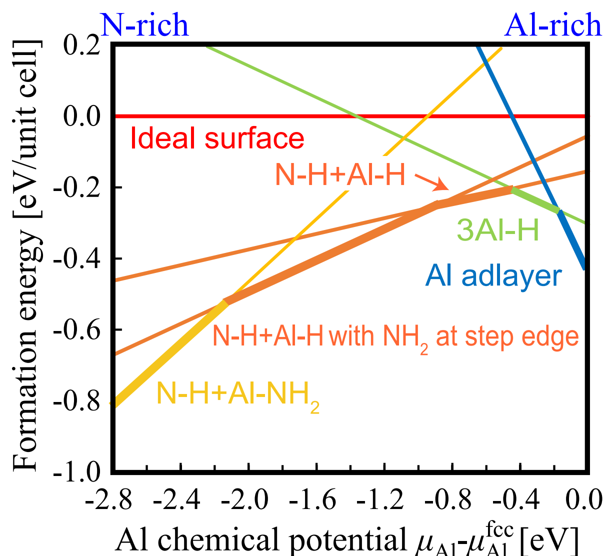

Fig. 2. Results of relative formation energy $E_{form}(\mu_{Al})$ using Eq. (1) for of various atomic configurations on vicinal AlN(0001) surfaces as a function of Al chemical potential μ_{Al} under H-rich condition. The origin of μ_{Al} corresponds to the energy of fcc Al. The value of hydrogen chemical potential μ_H corresponding to H_2 ambient at 76 Torr for 1370 K written as $\mu_H - \mu_{H_2} = -1.05$ eV (μ_{H_2} is the chemical potential per atom for single H_2 molecule at 0 K) is used. Note that only data for surface structures which can be stabilized in thermodynamically allowed range in μ_{Al} are shown. Geometries are shown in Fig. .1.

has the lowest under N-rich limit for $\mu_{Al} - \mu_{Al}^{fcc} \leqslant -2.15$ eV. Furthermore, 3Al-H and N-H + Al-H shown in Figs. 1(c) and 1(d) are stabilized for relatively Al-rich condition for $-0.90 \leqslant \mu_{Al} - \mu_{Al}^{fcc} \leqslant -0.20$ eV, respectively. Under Al-rich condition for $\mu_{Al} - \mu_{Al}^{fcc} \leqslant -0.20$ eV, Al adlayer shown in Fig. 1(b) is found to be stabilized. Therefore, five types of stable surface structures could appears depending on the growth condition of MOVPE. It is thus implied that the trend in the stable vicinal surface structure is similar to that of planar AlN(0001) surface [25]. Furthermore, the trend of stable atomic configurations on vicinal AlN(0001) surface is found to be similar to that of vicinal GaN(0001) surface [20]. In Figs. 1(e) and 1(f), hydrogen atoms partially terminate the dangling bonds located at bilayer step edge for the requirement of the EC rule [22].

Using the stable vicinal surfaces resolved in terms of the formation energies depicted in Fig. 2, the behavior of aluminum and nitrogen adatom adsorption is assessed for N-H + Al-H with NH_2 at the step edge and N-H + Al-NH_2. Since AlN is generally fabricated by the MOVPE growth under N-rich conditions, we take N-H + Al-NH_2 and N-H + Al-H with NH_2 at the step edge shown in Figs. 1(e) and 1(f) as prototypical vicinal surfaces during MOVPE, respectively. By comparing the value of Al chemical potential with the gas chemical potential of Al atoms [36], it is found that N-H + Al-H with NH_2 at the step edge and N-H + Al-NH_2 correspond to the reconstructed surfaces for low and high temperatures in MOVPE, respectively. Fig. 3 illustrates the positions of aluminum and nitrogen adatoms along the $[1\bar{1}00]$ direction and their energy profiles for N-H + Al-H with NH_2 at the step edge shown in Fig. 1(f). The results shown in Fig. 3 are applicable for the reconstruction under moderate N-rich ambient. According to the energy profile of aluminum adatom shown in Fig. 3(a), we find that the most stable adsorption site is located close to the step edge with $E_{ad} = -3.94$ eV. It is obvious that the adsorption energy closed to the step edge is much lower than those on terrace region and planar AlN(0001) surface of $E_{ad} = -1.89$ eV in previous calculations [24]. Therefore, the vicinal AlN(0001) surface preferentially incorporates the Al adatom at the step edge. The formation of two Al–N bonds with nitrogen atoms at the step edge indicated by black arrow in Fig. 3(a) is the origin of lower adsorption energy. Furthermore, we find a asymmetry in the energy barriers for downward and upward diffusion at the step edge, resulting in the appearance of ESB. We estimate the ESB (E_{ESB}) on the basis of the difference in barrier heights toward upper and lower terraces given by $E_{ESB} = E_{\downarrow} - E_{\uparrow}$, in which $E_{\downarrow}$ is barrier height for diffusing down and $E_{\uparrow}$ is barrier heights for diffusing up the step edge. The values of $E_{\downarrow}$ and $E_{\uparrow}$ obtained from Fig. 3(a) are 0.21 and 1.61 eV, respectively. For bilayer step edge, we can estimate the value of the ESB of -1.40 eV. The appearence of negative (inverse) ESB suggests the migration of aluminum adatoms from the upper terrace to the lower terrace is prominent compared with that from the lower terrace to the upper terrace.

On the basis of Fig. 3(b), it is found that the stable adsorption sites for the nitrogen adatom are located in the terrace. The adsorption energy at the most stable site is $E_{ad} = -4.11$ eV. The result of adsorption energy on vicinal surface is comparable to its counterpart on planar AlN(0001) surface of $E_{ad} = -4.17$ eV. The origin of low adsorption energy is attributed to the formation of three Al–N bonds with topmost Al atoms and single N–H bond. Furthermore, the energy barrier of N adatom diffusion in the terrace is found to be about 1.5 eV. Similar to the case of nitrogen adatoms on vicinal GaN(0001) surface [20], the adsorption results in N_2 molecule formation by the topmost hydrogen terminated N atom at the step edge. Thus, it is indicated that the migration of N adatom on vicinal surface is suppressed due to large diffusion barrier heights of ~ 1.5 eV and the formation of N_2 molecule. From the energy profile around the step edge, the values of $E_{\uparrow}$ and $E_{\downarrow}$ are found to be 1.54 and 1.44 eV, respectively. Therefore, the the ESB of -0.10 eV, which is much higher than the ESB for aluminum adatom, is estimated for bilayer step edge.

The calculated results for the positions of aluminum and nitrogen

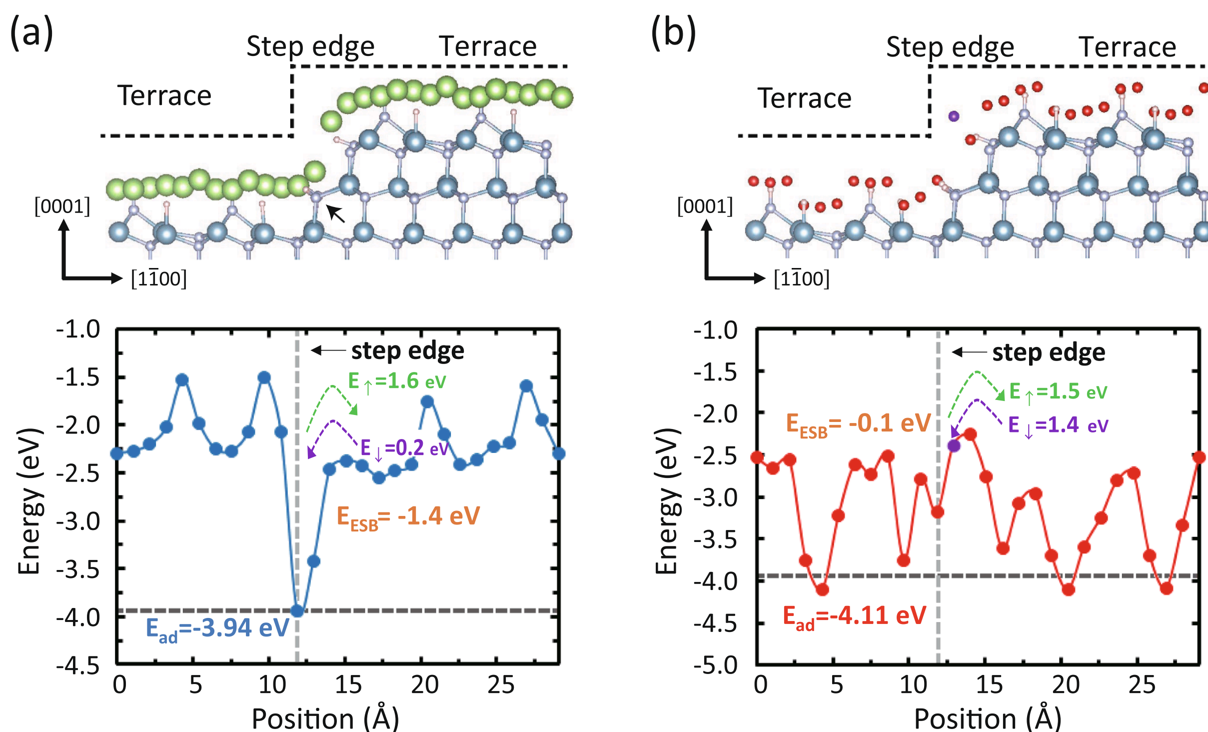

Fig. 3. Side views of positions of (a) aluminum and (b) nitrogen adatoms in the [1$\bar{1}$00] direction along with crresponding adsorption energy on vicinal AlN(0001) surface for N-H + Al-H with NH_2 at the step edge shown in Fig. 1(f). Notations of atoms in geometries are the same as those in Fig. 1. Adatoms of aluminum and nitrogen at each position are shown by green and red circles, respectively. The desorption as N_2 molecule is indicated by purple circle in the adsorption energy. Barrier height in energy for diffusing up (down) are described by $E_{\uparrow}$ ($E_{\downarrow}$) with green (purple) arrows. Black arrow in side view represents the N atoms which form two Al– N bonds at the most stable site for the Al adatom. Dashed horizontal lines in adsorption energies represent gas-phase chemical potential of Al and N atoms at 1 × 10^{-3} Torr for 1370 K..

adatoms along the [1$\bar{1}$00] direction and their energy profiles for N-H + Al-NH_2 in Fig. 1(e) are depicted in Fig. 4. The results shown in Fig. 4 are applicable for the surface reconstruction under N-rich limit. It is clearly seen in Fig. 4(a) that the location of most stable adsorption site for aluminum is close to the step edge with E_{ad}=−4.74 eV. The adsorption energy closed to the step edge is much lower than its counterparts on terrace region and planar AlN(0001) surface of E_{ad}=−2.03 eV. Therefore, the vicinal AlN(0001) surface preferentially incorporates the Al adatom at the step edge. Moreover, we find a asymmetry in the energy barriers for downward and upward diffusion at the step edge, resulting in the appearance of ESB. This indicates that analogous to the results of N-H + Al-H with NH_2 shown in Fig. 3(a) the vicinal surface of N-H + Al-NH_2 preferentially incorporates the Al adatom at the step edge. The formation of Al-NH_2 bond with pre-adsorbed N_2 in addition to two Al–N bonds indicated by black arrow in Fig. 4(a) is a physical origin of lower adsorption energy. From the energy profile around the step edge, the values of $E_{\uparrow}$ and $E_{\downarrow}$ are found to be 2.29 and 0.42 eV, respectively. Therefore, we can estimate the value of the ESB of −1.87 eV for the aluminum adadtom at bilayer step edge under N-rich limit. It is thus indicated that the amplitudes of the ESB for N-H + Al-NH_2 shown in Fig. 4(a) is larger than that for N-H + Al-H with NH_2 at the step edge shown in Fig. 3(a).

For the behavior of nitrogen adatom adsorption shown in Fig. 4(b), there are large energy differences of about 2 eV between the most stable site and the other metastable sites. It is found that the most stable adsorption site lies in the terrace region rather than step edge. The calculated adsorption energy at the most stable site is found to be −3.95 eV. From the energy profile around the step edge, the values of $E_{\uparrow}$ and $E_{\downarrow}$ are found to be 1.05 and 1.78 eV, respectively. The ESB for nitrogen adatom is thus estimated to be 0.73 eV, which is much higher than the ESB for aluminum adatom. However, the migration of nitrogen adatom on vicinal surface is suppressed owing to large diffusion barrier heights of ~ 2 eV. Similar to the nitrogen adatom for N-H + Al-H with NH_2 at the step edge, the adsorption results in N_2 molecule formation by the topmost hydrogen terminated N atom at the step edge. This indicates that N adatoms desorb from the step edges by N_2 desorption. Consequently, the behavior of the N adatom for N-H + Al-NH_2 is expected to be similar to that for N-H + Al-H with NH_2.

According to the adsorption energies of adatoms on vicinal AlN (0001) surfaces obtained in Figs. 3 and 4, it is suggested that the migration of aluminum adatoms is much faster than that of nitrogen adatoms. We thus deduce the growth mode such as step-flow and step bunching on the basis of the calculated results of aluminum adatoms shown in Figs. 3(a) and 4(a). Fig. 5 depicts the behavior of aluminum adatoms on vicinal AlN(0001) surfaces corresponding to the MOVPE growth at low and high temperatures. Here, the adsorption energies in the terraces in Fig. 5 are embed from the calculated results on planar AlN (0001) surface [24]. The appearance of inverse ESB at bilayer step edge shown in both Figs. 5(a) and 5(b) suggests that aluminum adatoms diffuse down the step edge from upper terrace toward lower terrace easily. This feature prevent step meandering [12], and is consistent with the AFM observations of step-flow and step-bunching without meandering at low and high temperature conditions in MOVPE [8]. However, it is difficult to understand the step-bunching at high temperature in MOVPE from the calculated ESB. One of possible explanations for the step-bunching at high temperature is low ESB in N-H + Al-NH_2 compared with that in N-H + Al-H with NH_2. Since the difference in ESB of 0.5 eV results in ~ 10 times larger probability for diffusing up the step in N-H + Al-H with NH_2 than N-H + Al-NH_2 at 1370 K, the growth condition dependence in diffusion behavior at the step edge could causes the difference in growth mode by growth condition. The adsorption of further aluminum and nitrogen atoms and clarifying the relationship between ESB and surface morphology on the basis of Burton-Cabrera-Frank theory [37] using calculated data should be examined for

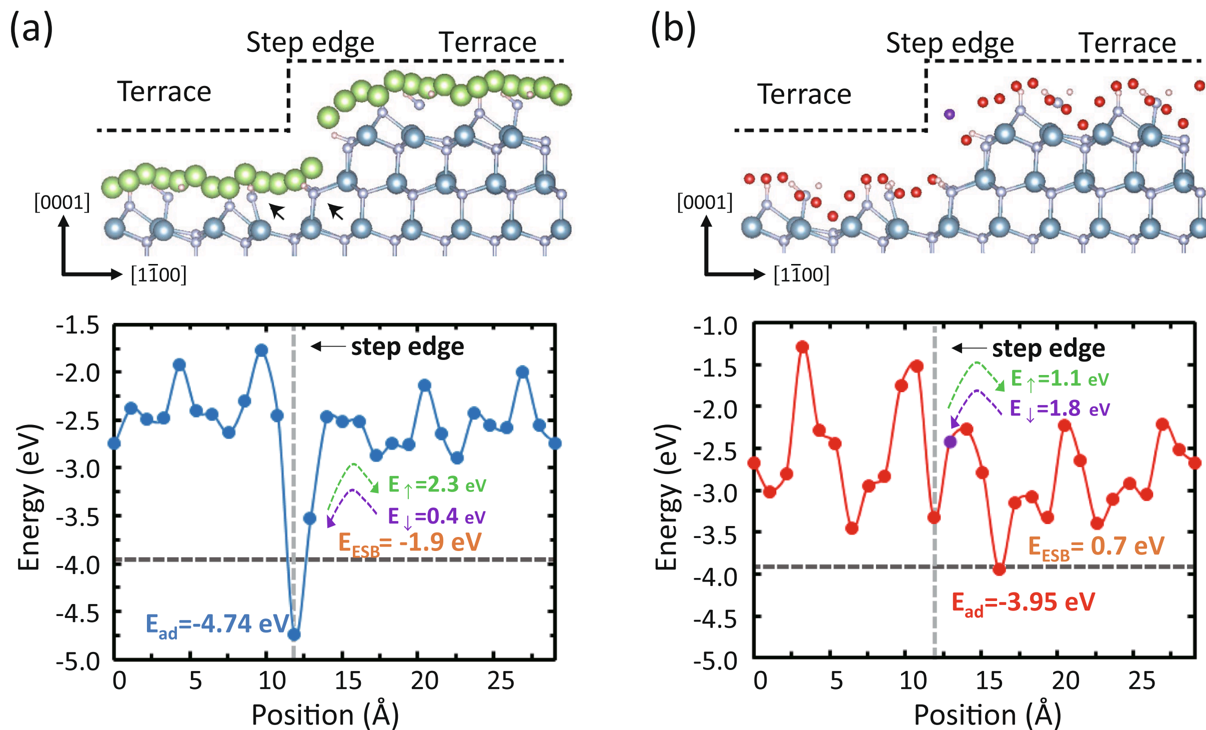

Fig. 4. Side views of positions of (a) aluminum and (b) nitrogen adatoms in the [1$\bar{1}$00] direction along with crresponding adsorption energy on vicinal AlN(0001) surface for N-H + Al-NH_2 shown in Fig. 1(e). Notations of atoms in geometries are the same as those in Fig. 1. Adatoms of aluminum and nitrogen at each position are shown by green and red circles, respectively. The desorption as N_2 molecule is indicated by purple circle in the adsorption energy. Barrier height in energy for diffusing up (down) are described by $E_{\uparrow}$ ($E_{\downarrow}$) with green (purple) arrows. Black arrows in side view represent pre-adsorbed NH_2 and N atoms which form Al-NH_2 and two Al–N bonds at the most stable site for the Al adatom. Dashed horizontal lines in adsorption energies represent gas-phase chemical potential of Al and N atoms at 1×10^{-3} Torr for 1370 K..

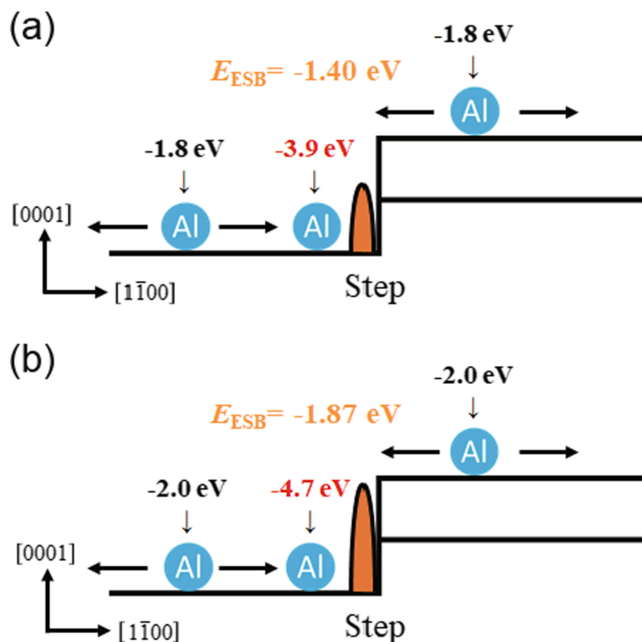

Fig. 5. Schematic views for the behavior of aluminum adatoms around bilayer step edges of (a) N-H + Al-H with NH_2 at the step edge and (b) N-H + Al-NH_2 for on vicinal AlN(0001) surfaces obtained from Figs. 3(a) and 4(a). The vicinal surfaces with N-H + Al-H with NH_2 at the step edge and N-H + Al-NH_2 correspond to low and high temperatures in MOVPE, respectively. Step edge and terrace regions are indicated by dashed stepwise lines. The adsorption energies at terrace are calculated by using conventional planar (2 × 2) slab models.

understanding of the morphology of vicinal AlN(0001) surfaces.

4. Conclusions

We have studied the adsorption behavior of adatoms on vicinal AlN (0001) surface during MOVPE growth from theoretical viewpoints by using *ab initio* calculations. From the calculated formation energies of vicinal surfaces with bilayer step edge for the [1$\bar{1}$00] direction, we have found the growth condition dependence of the stable structure of bilayer step edge. The surface terminated by nitrogen atoms with H and NH_2 (N-H + Al-NH_2) is found to be stable under N-rich limit, whereas the surface with hydrogen terminated N atoms (N-H + Al-H) with NH_2 at the step edge is favorable under moderate N-rich condition. Moreover, we have revealed specific adsorption behavior of aluminum and nitrogen adatoms caused by the bilayer step edge from the energy profiles of adsorption energy in the [1$\bar{1}$00] direction. Regardless of growth condition, the vicinal AlN(0001) surface preferentially incorporates the aluminum adatom at the bilayer step edge. The estimated ESB of aluminum adatom under N-rich limit and moderate N-rich condition are −1.9 and −1.4 eV, respectively, indicating that an inverse ESB exists on vicinal AlN(0001) surface during MOVPE. In contrast, the nitrogen adatom adsorbs on the terrace region rather than step edge. An N_2 molecule is found be formed by the adsorption at the step edge and desorbs from the surface. The morphology difference depending on the MOVPE growth condition could be attributed to the difference in ESB between the surfaces corresponding to high and low temperatures. Although further examination for the relationship between ESB and surface morphology in addition to the effects of other species such as AlH_x and NH_x (x = 1, 2, 3) [38,39] on the adsorption behavior are necessary, the results provide some insights for understanding and controlling the growth morphology of AlN.

CRediT authorship contribution statement

Toru Akiyama: Conceptualization, Methodology, Investigation, Resources, Writing – original draft, Writing – review and editing, Funding acquisition. **Takumi Ohka:** Formal analysis, Investigation, Data curation. **Katuya Nagai:** Formal analysis, Investigation, Data curation. **Tomonori Ito:** Conceptualization, Writing – review and editing, Funding acquisition.

Declaration of Competing Interest

The authors declare that they have no known competing financial interests or personal relationships that could have appeared to influence the work reported in this paper.

Acknowledgment

We would like to acknowledge financial supports by JSPS KAKENHI Grant Nos. JP16H06418, JP19K05268, and JP20K05324, CREST-JST Grant No. JPMJCR16N2. The work is also supported by the Collaborative Research Program of RIAM at Kyushu University. The computation in this work has been done using the facilities in Research Center for Computational Science (National Institutes of Natural Sciences) and Research Institute for Information Technology (Kyushu University).

References

[1] B. Heying, E.J. Tarsa, C.R. Elsass, P. Fini, S.P. DenBaars, J.S. Speck, J. Appl. Phys. 85 (1999) 6470.
[2] C. Adelmann, J. Brault, D. Jalabert, P. Gentile, H. Mariette, G. Mula, B. Daudin, J. Appl. Phys. 91 (2002) 9638.
[3] X.Q. Shen, M. Shimizu, H. Okumura, Jpn. J. Appl. Phys. 42 (2003) L1293.
[4] S. Vezian, F. Natali, F. Semond, J. Massies, Phys. Rev. B 69 (2004) 125329.
[5] G. Koblmueller, J. Brown, R. Averbeck, H. Riechert, P. Pongratz, J.S. Speck, Jpn. J. Appl. Phys. 44 (2005) L906.
[6] A.L. Corrion, F. Wu, J.S. Speck, J. Appl. Phys. 112 (2012) 054903.
[7] N.A.K. Kaufmann, L. Lahourcade, B. Hourahine, D. Martin, N. Grandjean, J. Cryst. Growth 433 (2016) 36.
[8] I. Bryan, Z. Bryan, S. Mita, A. Rice, J. Tweedie, R. Collazo, Z. Sitar, J. Cryst. Growth 438 (2016) 81.
[9] K. Bellmann, U.W. Pohl, C. Kuhn, T. Wernicke, M. Kneissl, J. Cryst. Growth 478 (2017) 187.
[10] G. Ehrlich, F.G. Hudda, J. Chem. Phys. 44 (1966) 1039.
[11] R.L. Schwoebel, E.J. Shipsey, J. Appl. Phys. 37 (1966) 3682.
[12] G.S. Bales, A. Zangwill, Phys. Rev. B 41 (1990) 5500.
[13] A. Pimpinelli, I. Elkinani, A. Karma, C. Misbah, J. Villain, J. Phys.-Condens. Matter 6 (1994) 2661.
[14] M.H. Xie, S.Y. Leung, S.Y. Tong, Surf. Sci. 515 (2002) L459.
[15] W. Hong, H.N. Lee, M. Yoon, H.M. Christen, D.H. Lowndes, Z.G. Suo, Z.Y. Zhang, Phys. Rev. Lett. 95 (2005) 095501.
[16] Y. Kangawa, T. Akiyanama, T. Ito, K. Shiraishi, T. Nakayama, Materials 6 (2013) 3309.
[17] T. Akiyama, et al., in: T. Matsuoka, Y. Kangawa (Eds.), Epitaxial Growth of III-Nitride Compounds, Springer, Berlin, 2018.
[18] T. Akiyama, T. Ohka, K. Nakamura, T. Ito, J. Cryst. Growth 532 (2020) 125410.
[19] T. Akiyama, T. Ohka, K. Nakamura, T. Ito, Jpn. J. Appl. Phys. 59 (2020) SGGK03.
[20] T. Ohka, T. Akiyama, A.-M. Pradipto, K. Nakamura, T. Ito, Cryst. Growth Des. 20 (2020) 4358.
[21] K. Shiraishi, J. Phys. Soc. Jpn. 59 (1990) 3455.
[22] M.D. Pashley, K.W. Haberern, W. Friday, J.M. Woodall, P.D. Kirchner, Phys. Rev. Lett. 60 (1988) 2176.
[23] H. Suzuki, R. Togashi, H. Murakami, Y. Kumagai, A. Koukitu, Jpn. J. Appl. Phys. 46 (2007) 5112.
[24] T. Akiyama, K. Nakamura, T. Ito, Appl. Phys. Lett. 100 (2012) 251601.
[25] T. Akiyama, D. Obara, K. Nakamura, T. Ito, Jpn. J. Appl. Phys. 51 (2012) 018001.
[26] Y. Seta, A.-M. Pradipto, T. Akiyama, K. Nakamura, T. Ito, A. Kusaba, Y. Kangawa, Jpn. J. Appl. Phys. 58 (2019) SC1014.
[27] J.P. Perdew, K. Burke, M. Ernzerhof, Phys. Rev. Lett. 77 (1996) 3865.
[28] N. Troullier, J.L. Martins, Phys. Rev. B 43 (1991) 1993.
[29] D. Vanderbilt, Phys. Rev. B 41 (1990) 7892.
[30] J. Yamauchi, M. Tsukada, S. Watanabe, O. Sugino, Phys. Rev. B 54 (1996) 5586.
[31] H. Kageshima, K. Shiraishi, Phys. Rev. B 56 (1997) 14985.
[32] W.M. Yim, E.J. Stofko, P.J. Zanzucchi, J.I. Pankove, M. Ettenberg, S.L. Gilbert, J. Appl. Phys. 44 (1973) 292.
[33] Y. Yoshimoto, S. Tsuneyuki, Surf. Sci. 514 (2002) 200.
[34] J. Yamauchi, Y. Yoshimoto, Y. Suwa, Appl. Phys. Lett. 99 (2011) 191901.
[35] D.D. Wagman, W.H. Evans, V.B. Parker, R.H. Schumm, I. Halow, S.M. Bailey, K. L. Churney, R.L. Nuttall, J. Phys. Chem. Ref. Data 11 (1982) 2.
[36] Y. Kangawa, T. Ito, A. Taguchi, K. Shiraishi, T. Ohachi, Surf. Sci. 493 (2001) 178.
[37] W.-K. Burton, N. Cabrera, F. Frank, Philos. Trans. R. Soc. Lond. Ser. A: Math. Phys. Eng. Sci. 243 (1951) 299.
[38] K.M. Bui, J.-I. Iwata, Y. Kangawa, K. Shiraishi, Y. Shigeta, A. Oshiyama, J. Phys. Chem. C 122 (2018) 24665.
[39] K.M. Bui, J.-I. Iwata, Y. Kangawa, K. Shiraishi, Y. Shigeta, A. Oshiyama, J. Cryst. Growth 507 (2019) 421.